Effects of Casting Solvents on the Formation of Inverted Phase in Block Copolymer Thin Films

Haiying Huang, Zhijun Hu, Yongzhong Chen, Fajun Zhang, Yumei Gong, and Tianbai He*

State Key Laboratory of Polymer Physics and Chemistry, Changchun Institute of Applied Chemistry, Chinese Academy of Sciences, Changchun 130022, P. R. China

Chi Wu

Department of Chemistry, The Chinese University of Hong Kong, Shatin. N. T., Hong Kong

Received January 20, 2004; Revised Manuscript Received June 12, 2004

ABSTRACT: Previously, an inverted phase (the minority blocks comprising the continuum phase) was found in solution-cast block copolymer thin films. In this study, the effect of casting solvents on the formation of inverted phase has been studied. Two block copolymers, poly(styrene-*b*-butadiene) (SB) (M_w = 73 930 Da) and poly(styrene-*b*-butadiene-*b*-styrene) (SBS) (M_w = 140 000 Da), with comparable block lengths and equal polystyrene (PS) weight fraction (∼30 wt %) were used. The copolymer thin films were cast from different solvents, toluene, benzene, cyclohexane, and binary mixtures of benzene and cyclohexane. Toluene and benzene are good solvents for both PS and PB, but have a preferential affinity for PS, while cyclohexane is a good solvent for PB but a Θ solvent for PS (T_Θ = 34.5 °C). The differential solvent affinity for PS and PB was estimated in terms of a difference between the polymer−solvent interaction parameter, χ, for each block. Under an extremely slow solvent evaporation rate, the time-dependent phase behavior during such a solution-to-film process was examined by freeze-drying the samples at different stages, corresponding to different copolymer concentrations, φ. Our results indicate that the slight interaction difference between solvent and each block influences the effective volume fraction of each domain and drives the solution to form a transient inverted phase at the early stage of the microphase separation.

Introduction

The microdomain structure in block copolymer thin films has been investigated extensively in experiments,[1−20] theory,[21−23] and simulation.[24−28] An interesting finding is that the resulting morphologies are not restricted to the equilibrium state in the bulk, since the additional constraints, such as interfacial interactions, film thickness, and different film preparation conditions, play an important role. Because of such complex interplay of different parameters in the films, it is difficult to completely understand their formation and transition mechanism. Therefore, the studies of phase behavior in thin films continue to be a fascinating and stimulating area.

In recent years, there are many literatures concentrated on studying the evolution and orientation of microstructures in thin films by applying external fields.[7−10,16,19,20,29,30] Among them, solvent evaporation is a simple and direct route in controlling the ordering and orientation of the microdomain morphology of block copolymers. In this procedure, the solvent imparts mobility to the system, enabling alignment of the microdomains without any thermal treatment. Kim and Libera[7] used the solvent evaporation rate to manipulate cylinder orientation in solution-cast films. Russell and co-workers[20] recently showed that, by controlling the rate of solvent evaporation or solvent annealing, the highly oriented cylindrical domains are produced that span the entire film thickness with long-range lateral order. In our previous report,[31] we employed the same approach to investigate the evolution of the microstructures in solution-cast films of one poly(styrene-*b*-butadiene-*b*-styrene) (SBS) triblock and four poly(styrene-*b*-butadiene) (SB) diblock copolymers having nearly equal PS weight fractions (about 30 wt %) as a function of solvent evaporation rate. The intriguing finding is that we uncovered unconventional inverted phase consisting of spheres or cylinders of the majority block (PB) in a matrix of the minority block (PS). We conclude that the formation of inverted phase has little bearing on the chain architecture. Moreover, for SB diblock copolymers, the results indicated that there is a threshold molecular weight or range of molecular weight below which the unusual inverted phase is accessible when a faster evaporation rate was applied. Although by performing numerical calculations for free energy of diblock and triblock cylinders, a mechanism based on kinetic effect is proposed to explain the origin of inverted phase, an in-depth understanding of their formation is far more complete. Since the observation differs from numbers of publications dealing with cylinder forming block copolymer thin films, many aspects related to their formation still need to be further investigated.

In contrast to the melt phase map, where the shorter blocks form the minor domains of a given morphology, block copolymer solutions allow the possibility of forming inverted phase in which the swollen shorter block plus solvent forms the major domain.[32] Moreover, in block copolymer solutions, the phase behavior is more complicated than those in melts due to the additional role played by solvent selectivity.[32−36] Hence, in the A−B block−solvent system, besides the *f* (the volume fraction of minority block), *N* (the total degree of polymerization),

* To whom correspondence should be addressed. E-mail: tbhe@ciac.jl.cn.

10.1021/ma0498621 CCC: $27.50
Published on Web 07/27/2004

φ (the volume fraction of the polymer in solution), and χ_{AB} (Flory−Huggins interaction parameter between A and B), the phase behavior depends strongly on the polymer−solvent interaction parameter, χ_{AS} and χ_{BS}, where "S" indicates solvent. For a given copolymer composition *f*, if the solvent is neutral or good, the mean-field order−order transitions (OOT) and order−disorder transitions (ODT) can be obtained from the melt phase map by replacing $\chi_{AB}N$ with $\phi\chi_{AB}N$ in the concentrated regime and $\phi^{1.59}\chi_{AB}N$ in the semidilute regime.[37,38] But for block copolymer in selective solvents, the phase behavior has only recently been treated theoretically. Banaszak and Whitmore[39] presented the first self-consistent mean-field (SCMF) theory for such systems to study the lamellar mesophase in slightly selective solvents. Huang and Lodge[40] employed the SCMF approach to systematically examine the phase behavior of block copolymers in the presence of a solvent, which is a function of solvent selectivity, temperature, copolymer concentration, composition, and molecular weight. On account of these theoretical studies, the understanding of microstructures of block copolymer films prepared from solutions has attracted increasing attention[41−48] because the organized structure observed in the solid thin film is greatly influenced by the nature and the concentration of the solvent. This also reminded us that the nature of solvent used in the casting process may in part be responsible for the formation of inverted phase, since the perfectly nonselective solvent is unlikely and rarely found for real block copolymer systems and the small degree of preferential affinity that will generally exist for a copolymer in a solvent good for both blocks.[49,50] Motivated by such idea, therefore, in the present paper, our research will focus on exploring the solvent effect on the formation of inverted phase. By properly controlling the preparation conditions, we will show that the formation of inverted phase strongly depends on the nature of the solvent and on the block copolymer solution concentration, φ.

Here, we will describe a more effective freeze-drying method, where the microdomain structure in solution is frozen-in at different time during the process of extremely slow evaporation rate. This chosen procedure had two aspects. First, in such extremely slow evaporation conditions, the kinetically controlled inverted phase will disappear, since block polymer chains have enough time to rearrangement and only one expected the ultimate equilibrium state—the cylindrical normal phase can be reached finally. Second, during the evaporation of solvent the concentration of polymer solution gradually increases; it must experience a process from dilute solution to concentrated solution before formation of solid thin films. In this way, the morphologies frozen at different time correspond to kinetic frozen-in phase structures at qualitatively different block copolymer concentration; φ, i.e., the morphology observed in the solution-cast films can be considered to be the memory of the domain structure which existed in the solution.

The system chosen for the current study is SB diblock (M_w = 73 930 Da) and matched SBS triblock (M_w = 140 000 Da) copolymers having equal polystyrene (PS) weight fractions (about 30 wt %). Three representative solvents—toluene, benzene, and cyclohexane—were employed. Both toluene and benzene are good solvents for PS and PB, but preferential affinity for PS, while cyclohexane is a good solvent for PB and a Θ solvent for PS (T_Θ = 34.5 °C). In addition, benzene and cyclohexane as model solvents having the opposite affinity for the PS and PB, and the films cast from their binary solvent mixture with different volume ratio are also comparatively investigated for a given time, which can help us to study the solvent effect in a systematic way. We should emphasize that the phase behavior studied here is far more different from the system that using the highly selective solvents, $\chi_{AS} \ll \chi_{BS}$, which leads to micellization with the micellar cores formed by the insoluble domain.

Table 1. Characteristics of Casting Solvents

	δ (J/cm^3)$^{1/2}$ solubility parameter[a]	V (mL/mol) molar vol[b]	T_b boiling temp[b]
toluene	18.2	106.3	111
benzene	18.8	88.9	80
cyclohexane	16.8	108.0	81

[a] Obtained from *Polymer Handbook*.[52] [b] Obtained from *Properties of Polymers*.[53]

Table 2. Vapor Pressures of Benzene near the Room Temperature

temperature (°C)	vapor pressure (mmHg)
15.4	60
26.1	100
42.2	200

Table 3. Vapor Pressures of Cyclohexane near the Room Temperature

temperature (°C)	vapor pressure (mmHg)
14.7	60
25.5	100
42.0	200

Experimental Section

Materials. The sample poly(styrene-*b*-butadiene-*b*-styrene) (SBS) triblock (M_w = 140 000 Da) and the matching (styrene-*b*-butadiene) SB diblock (M_w = 73 930 Da) copolymers having equal polystyrene (PS) weight fraction (about 30 wt %) were purchased from Aldrich Chemical Co, and their characterizations have been fully described in our previous paper.[31] In the bulk, both samples adopt hexagonal microstructures with PS cylinders embedded in a PB matrix.[51] A total of three solvents, toluene, benzene, and cyclohexane, were employed to dissolve both block copolymers. The characteristics of the three solvents are listed in Table 1.[52,53] Table 2 and Table 3 list the vapor pressures of the benzene and cyclohexane near room temperature,[54] showing that benzene and cyclohexane have equal volatility. In addition, the binary solvent mixtures of benzene and cyclohexane were made up by volume are also be used to dissolve SB diblock copolymer. Each solvent mixture was prepared volumetrically at room temperature, ignoring possible volume changes upon mixing.

Sample Preparation. For all the solutions the initial polymer concentration was 0.5 wt %. A 20 μL pipet was used to cast equal-sized droplets of the solutions onto carbon-coated mica, leaving fine rings of copolymer droplets. In the experiment, no matter the films cast from what solvent, the evaporation condition was fixed at extremely slow evaporation conditions. This was achieved by making the solution-cast films exposed to corresponding solvent vapor of ~95% saturation (cast a few drops of solution around the substrate at the initial stages) in a cylinder container completely covered with a lid. Under these conditions, solvent could only escape through the small gap between the container and its lid. In turn, we will select different time (*t*) to freeze-in the transient microdomain structures during such a slow solvent evaporation process, i.e., the solution-to-film process. When the time was reached, the lid was removed quickly and liquid nitrogen was poured into the container directly, so that it was frozen in a fraction of a second. Subsequently, the frozen samples were put into

Table 4. Polymer-Solvent Interaction Parameters (χ) Calculated from Different Pairs of Polymers and Solvents

	toluene	benzene	cyclohexane
PS	0.3469	0.3414	0.5322[a]
PB	0.4018	0.4563	0.3417

[a] Cyclohexane is a Θ solvent for PS at 34.5 °C, $\chi_{PS-cyclohexane} = -0.556 + 324.3/T$;[58] if T = 298 K (at room temperature), $\chi_{PS-cyclohexane} = 0.5322$.

another airtight chamber connected with a pump; the frozen solvent was then sublimed in a vacuum (10^{-4} Torr). To keep the samples in the frozen state and avoid the influence of evaporation on the frozen films, the airtight chamber will be immersed in liquid nitrogen existed in the whole experiment process. During the experiment procedure, no sign of dewetting was detected within the experimental time window. After completely dried, the average thickness of the deposited film was ~600 nm. To most accurately compare the microstructures of various samples from different time and different nature of solvents, all the experiments proceeded together. For example, when comparing the influence of different nature of solvents on the resulting microstructure for SB diblock copolymer, each sample was prepared in parallel at given time.

Instruments. The tapping-mode atomic force microscopy (TM-AFM) measurements were carried out in a NanoScope IIIa scanning probe microscope (Digital Instruments Inc.). As a widely used tool, AFM provides the direct visualization of the microstructures, and the measurements can cover the whole film thickness. During imaging, the AFM cantilever (spring constant between 1.5 and 3.5 N m^{-1}) was driven to oscillate at ~400 kHz, close to the cantilever's resonant frequency. The microscope was operated at moderate tapping so the glassy PS domains appear dark and the rubbery PB domains appear bright in the images.[55,56]

Transmission electron microscopy (TEM) experiments were performed on a JEOL 2010 electron microscope, operating at 200 kV accelerating voltage for a bright field mode. After AFM measurements, the same samples were separated from the mica surface by immersing in a distilled water bath. The carbon layer floats on the water bath, allowing the polymer and its carbon support to be picked up on standard mesh TEM grids. To enhance the contrast between PS and PB phases, the specimens were stained with osmium tetraoxide (OsO_4) for ~30 min prior to observation. Since OsO_4 selectively reacts with the double bonds in PB, the PB phase appears dark and the PS phase appears bright in the micrographs. Within a given specimen, some thickness variations were observed (tend to be thicker on the edge of the film and thinner in the center). Because the thicker part cannot transmit the electron beam, we chose regions that are transmitting to the electron beam (~150−400 nm) for examination.

Results and Discussion

For a given system a solvent that is good for one block can be classified as neutral, slightly selective, or strongly selective, according to whether it is good, near Θ, or a nonsolvent for the other block. This relative affinity of solvent for each block can be governed by polymer−solvent interaction parameter, $\chi_{ps} = V_s(\delta_s - \delta_p)^2/RT + 0.34$,[52] where V_s is the molar volume of the solvent, R is the gas constant, T is the temperature, and δ_s and δ_p are the solubility parameters of the solvent and polymer, which are also convenient to use as a means of estimating the compatibility between polymer and solvent. In present work, for PS and PB, the solubility parameters are reported as $\delta_{PS} = 9.1$ $(cal/cm^3)^{1/2} = 18.6$ $(J/cm^3)^{1/2}$ and $\delta_{PB} = 8.3$ $(cal/cm^3)^{1/2} = 17.0$ $(J/cm^3)^{1/2}$, respectively.[57] The calculated polymer−solvent interaction parameters (χ) for different pairs of polymers and solvents at room temperature are listed in Table 4. According to the Flory−Huggins theory criterion, polymer and solvent are completely miscible over the entire composition range when the obtained value $\chi < 0.5$. Hence, the solvents used in this work should be solvents, which are good for one block and either good or near Θ for the other. However, for each solvent there still exists small difference in polymer−solvent interaction parameters between PS and PB blocks, which is concerned with the difference in affinity of the solvent to the polymer components. Accordingly, toluene and benzene as nominally neutral solvent has preferential affinity for the minority PS block; on the contrary, cyclohexane has preferential affinity for the majority PB block.

Table 5. Phase Structures of the Block Copolymer Films Cast from Toluene as a Function of Time under the Extremely Slow Evaporation Rate[a]

	time (t)					
	1.5 h	2.0 h	2.5 h	3.0 h	3.5 h	~days
SBS	IS	IC and NC	NC	NC	NC	NC
SB	IS	IS and IC	IS and IC	IC	NC	NC

[a] IS = inverted sphere, IC = inverted cylinder, NC = normal cylinder.

In Table 5, we summarize the phase behaviors of SBS triblock and SB diblock copolymer films cast from toluene freeze-dried at different time, namely, at different block copolymer solution concentrations, φ. Despite the different time of microdomain structure formation, both SBS and SB copolymers exhibit qualitatively the same inverted-to-normal phase transitions as a function of time. As shown, for SBS the inverted to normal phase transition moment appeared at $t \sim 2.0$ h, while for SB2 this moment may exist between $t \sim 3.0$ h and $t \sim 3.5$ h. As time progressed, the normal phase was consistently observed for the two block copolymers. Next, we will present TM-AFM phase-contrast images of SBS and SB samples freeze-dried at typical times to justify our observations in Table 5.

Figure 1 displays the TM-AFM images of thin-films of SBS and SB copolymers. For the SBS triblock copolymer films, the microstructure (Figure 1a−c) changes from inverted PB spheres (i.e., PB spheres in a PS matrix) to normal PS cylinders (i.e., PS cylinders in a PB matrix) and traverses a hybrid structure showing the coexistence of the inverted PB cylinders (i.e., PB cylinders in a PS matrix) and normal PS cylinders. For SB diblock copolymer films, the microstructure (Figure 1d−f) changes from inverted PB spheres to definitely inverted PB cylinders and finally to normal PS cylinders, but the apparent coexistence of inverted and normal phase structures was not observed for a given time. Though we designed a new route to control the phase behaviors of SBS and SB block copolymers, the phase structures revealed by TM-AFM are consistent with those by TM-AFM shown in our previous study, subjected to different evaporation rates.[31] Moreover, both block copolymers have the same packing characteristics, since in comparison with the sequence structure of SBS triblock, the SB diblock approximately fulfills the relationship of $S(^1/_2B)$;[31] i.e., the block length of the middle block (PB) of the SBS triblock is twice that of the PB block of SB diblock whereas the block length of each end block (PS) of the triblock is the same as that of the diblock. It should be mentioned that for each sample, within the measurements (include edge and center of the films), we do not observe the significant changes of the morphologies even

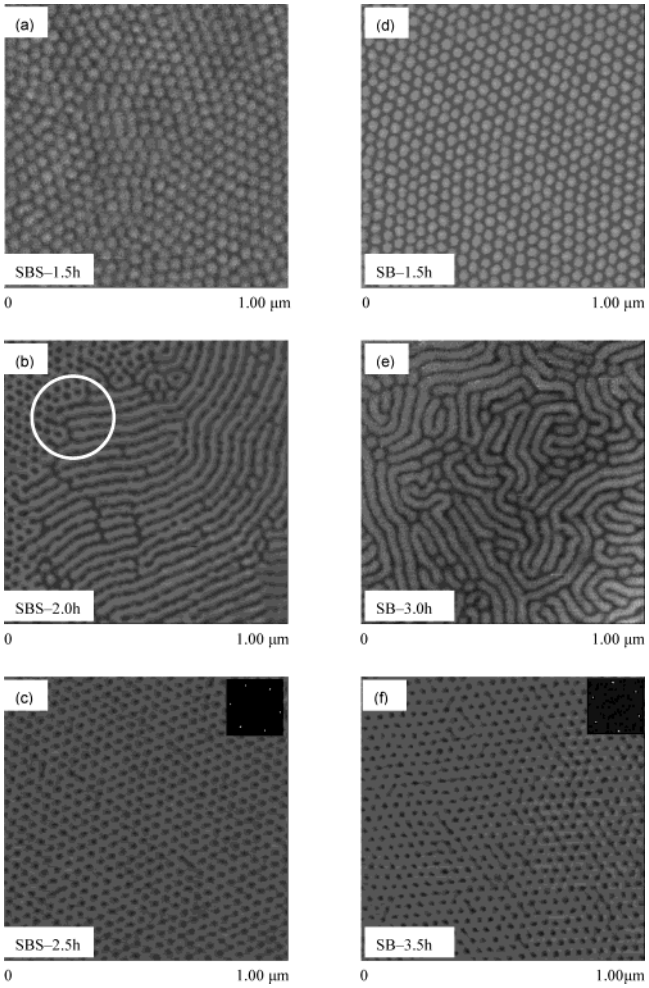

Figure 1. Tapping mode AFM phase images obtained from solution-cast (a)−(c) SBS triblock copolymer films and (d)−(f) SB diblock copolymer films freeze-dried at different times as indicated. The white circles in (b) illuminate the boundary between the inverted and normal phase.

though there is some thickness variation in the films. Therefore, the phase behaviors of samples formed under different conditions shown in Figure 1 are representative and reliable.

As mentioned above, the control with different time leads to frozen-in microstructures corresponding to different block copolymer solution concentration, φ. It is clear from the results shown that the inverted phase strongly depends on the copolymer solution concentration, φ. As a time-dependent process, the solution-cast film is first solvent-rich and hence disordered. Then as the concentration of the copolymer gradually increases, at a critical solution concentration the phase separation starts to take place, and the morphology is formed. Thus, the inverted phase captured at short time scale indicates that the inverted phase very likely formed at aforesaid moment before it reached their thermodynamic equilibrium state. Recently, Kim et al.[20] demonstrated that the solvent evaporation in thin films is unidirectional with a gradient in solvent concentration normal to the surface. They considered that at the beginning of the solvent evaporation the microphase separation occurs only at the surface, and the interior of the film is still disordered due to the higher concentration of solvent; further solvent evaporation is able to cause an ordering front to propagate through the film. Our system, however, showed that during the process of solvent evaporation the microdomain structures, which exist in solution, were preserved in solution-cast films by rapid freezing. It means that the microdomain structures appear not only at the surface but also in the interior of the films. Though we have not given cross-sectional views of the specimen in the thickness direction, according to the experimental evidence available at present, and previous cross-sectional views of the SBS films obtained at faster evaporation rate (corresponding to smaller, φ),[9] we may deduce that the microstructures presented here are not merely a surface structure but persist down to the bulk. As a matter of fact, in block copolymer solutions, the inverted to normal phase transition has been theoretically examined by Huang and Lodge.[40] But such transitions must be related to the solvent selectivity. For example, they calculate the two-dimensional phase map for AB block copolymer solution in terms of φ and f when $\chi_{AB}N = 45$, $\chi_{AS} = 0.6$, and $\chi_{BS} = 0.4$ (Figure 12 of ref 40). As φ decreases, the inverse hexagonal cylinders C_A and bcc spheres S_A are observed before the disordered phase is reached for the system $0.5 < f < 0.746$. Nevertheless, such transition from inverted to normal phase is more favored when the solvent is strongly selective for the minority block, which was also experimentally observed in recent study.[32,36] Therefore, it is very likely that the small degree of preferential affinity of toluene for minority PS block induces formation of the inverted phase in solution-cast films, even though the difference between the two polymer−solvent interaction parameters is small.

To further clarify our point of view and determine the nature of solvent on the formation of inverted phase, experiments were conducted infilms cast from benzene (designated as $V_b/V_c = 10/0$), cyclohexane (designated as $V_b/V_c = 0/10$), and their binary solvent mixtures with different volume ratio: $V_b/V_c = 7/3$, 5/5, 3/7. As model solvents, benzene and cyclohexane have the opposite affinity for PS and PB blocks. For their binary solvent mixture, in the simplest theory, it can be treated as a hypothetical single solvent, characterized by $\delta_{mix} = \sum\phi_i\delta_i$,[52] where ϕ_i is the volume fraction in the mixture. With changing volume ratio from 10/0, 7/3, 5/5, 3/7, to 0/10, the solubility parameters of binary solvent mixture will change from 18.8, 18.2, 17.8, 17.4, to 16.8 $(J/cm^3)^{1/2}$, respectively. Since a good solvent will have a solubility parameter positioned closer to that of the solute ($\delta_{PS} = 18.6$ $(J/cm^3)^{1/2}$ and $\delta_{PB} = 17.0$ $(J/cm^3)^{1/2}$), by varying the two solvent mixture compositions, the solvent affinity for PS will decrease; on the contrary, it will increase for PB. Hence, it is interesting to note whether a progressive change can occur with films cast from different nature of solvents. On the other hand, since the vapor pressures of benzene and cyclohexane are higher than toluene at room temperature, benzene and cyclohexane should be more volatile than toluene at the same evaporation condition. Here, the comparison study is concentrated on the films freeze-dried at $t = 1.0$ h because the phase structures captured at that time can be comparable with films cast from toluene freeze-dried at $t = 1.5$ h which form the inverted spheres.

Figure 2a−e shows the TM-AFM phase-contrast images of SB diblock copolymer films cast from benzene, cyclohexane, and their binary solvent mixtures freeze-dried at $t = 1.0$ h. For the film cast from pure benzene, the inverted PB spheres were obtained (Figure 2a). For the film cast from binary solvent mixture with volume

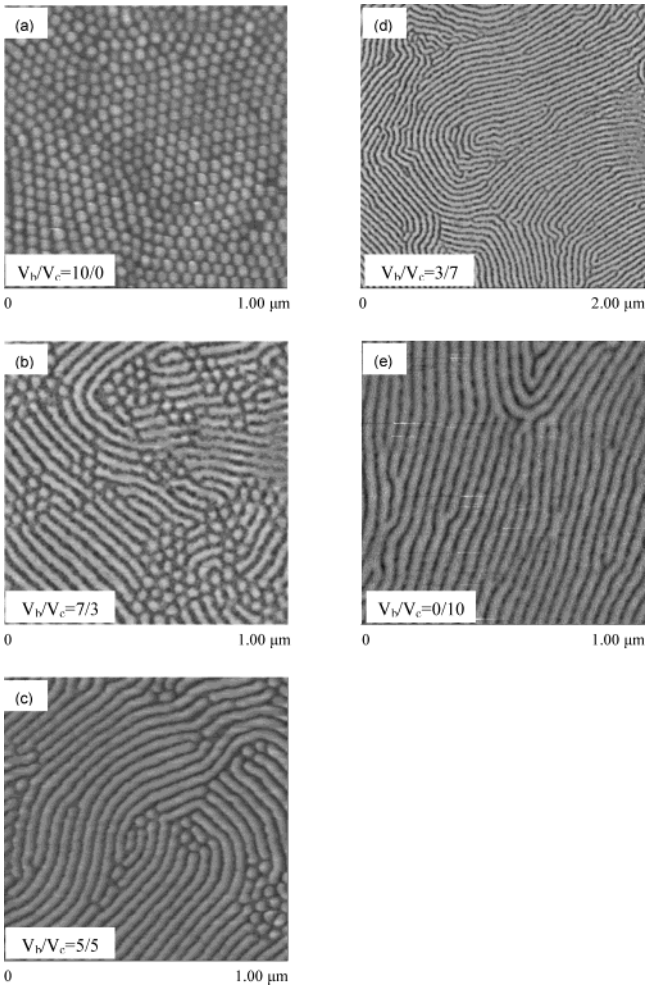

Figure 2. (a−e) Tapping mode AFM phase images of SB diblock copolymer films cast from benzene, cyclohexane, and their binary solvent mixtures with different volume ratio freeze-dried at $t = 1.0$ h as indicated.

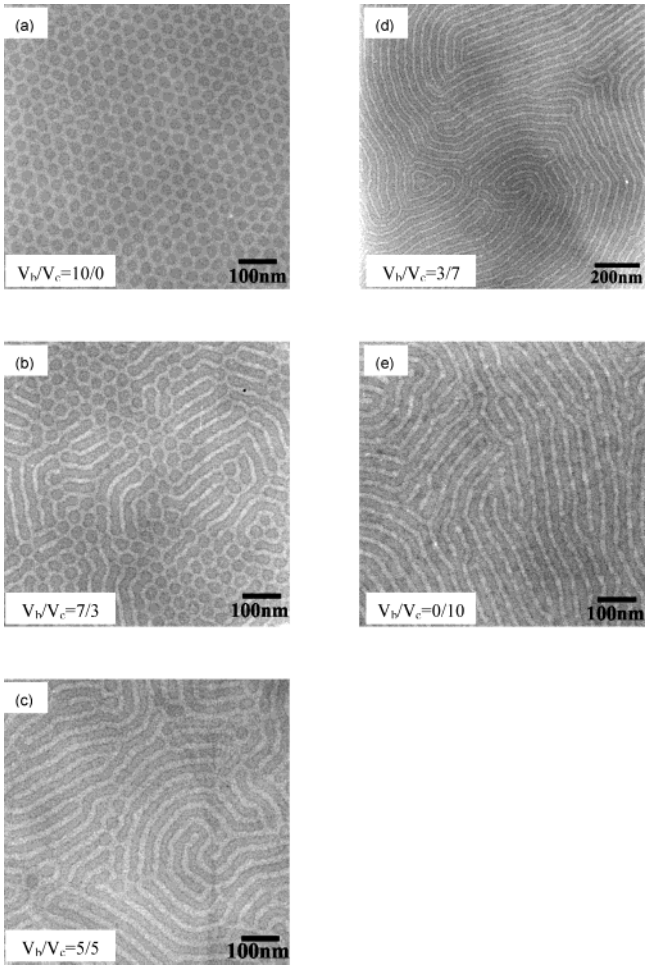

Figure 3. (a−e) Plain-view bright-field TEM micrographs of the same SB diblock copolymer films corresponding to Figure 2.

ratio $V_b/V_c = 7/3$ and 5/5, the inverted phase is still the dominant structure, which seen clearly in Figure 2b (PB spheres and cylinders in a PS matrix) and Fgure 2c (PB cylinders in a PS matrix). With a further decrease in the benzene content ($V_b/V_c = 3/7$), the hybrid structure showing coexistence of the normal and inverted planar cylinders was found (Figure 2d), which was judged by the disclination defects.[31] Finally the normal PS cylinders were obtained in film cast from pure cyclohexane (Figure 2e). Figure 3a−e displays the BF-TEM images that are consistent with the corresponding TM-AFM images in Figure 2a−e, respectively, which evidently show that our assignment of phase structures in TM-AFM phase images was correct. For SBS, Figure 4 and Figure 5 show the TM-AFM and BF-TEM images of SBS films cast from pure benzene and cyclohexane under the same conditions as that of SB diblock copolymer films. As is clearly seen in Figure 4 and Figure 5, the inverted PB spheres (Figures 4a and 5a) and normal PS cylinders (Figures 4b and 5b) were also presented in films cast from pure benzene and cyclohexane, respectively. In contrast to the phase structures of SB triblock and SB diblock films cast from toluene freeze-dried at $t = 1.5$ h (Figure 1a and 1d), the inverted PB spheres were also observed in film cast from pure benzene freeze-dried at $t = 1.0$ h (Figures 2a and 3a, Figures 4a and 5a). Since benzene is a chemically similar solvent to toluene and preferential affinity for minority PS block, it is not surprising that films cast from the two solvents exhibit the similar phase behavior. In the order of decreasing the solvent affinity for minority PS block, notable changes occurred that inverted phase structures gradually disappeared, which can be seen clearly in films cast from pure cyclohexane (Figures 2e and 3e, Figures 4b and 5b). The results described above demonstrated that the evolution of the microdomain structures in solution-cast films is strongly dependent on the nature of the solvent. It indicates that the preferential affinity of solvent for minority PS block, indeed, has a major effect on the formation of inverted phase.

As far as the morphologies of thin films is concerned, cylinder-forming block copolymers exhibit more complex phase behaviors, which mainly rely on the film thickness and the surface−polymer interactions. Besides cylinders align perpendicular and parallel to the substrate,[6,7] a variety of thin film structures have been reported on, including a laterally homogeneous wetting layer,[2] spherical microdomains,[3] and a perforated lamella (PL).[3] In a very recent study, Knoll et al.[19] has performed a most comprehensive investigation of microdomain structures of cylinder-forming SBS triblock copolymer thin films as a function of film thickness and polymer concentration, which controlled by the solvent vapor pressure (chloroform). Within the observations, a perforated lamella was found at high polymer concentrations and at a film thickness close to one or two layers of cylinders. It is interesting to consider whether

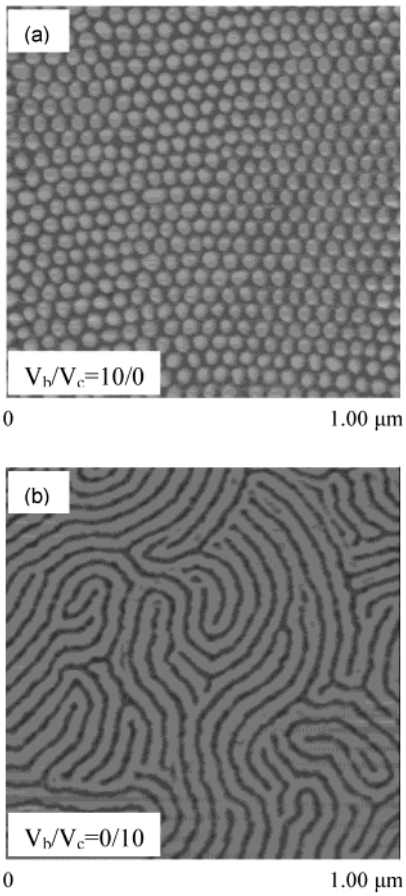

Figure 4. Tapping mode AFM phase images obtained from solution-cast SBS triblock copolymer films freeze-dried at t = 1.0 h: (a) cast from benzene (V_b/V_c = 10/0); (b) cast from cyclohexane (V_b/V_c = 0/10).

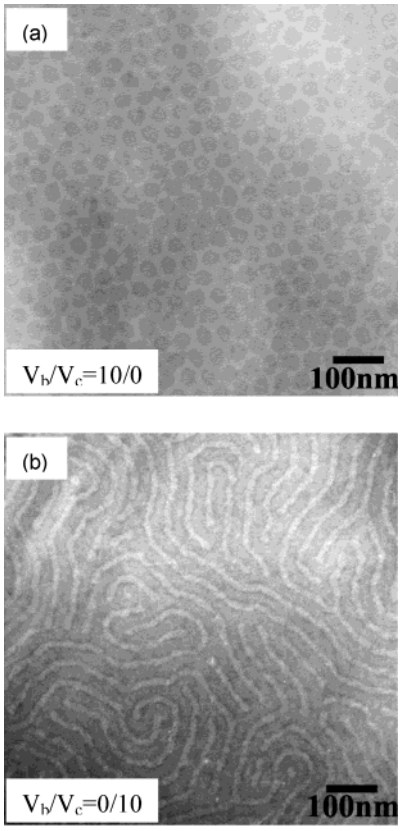

Figure 5. Plain-view bright-field TEM micrographs of the SBS triblock copolymer films freeze-dried at t = 1.0 h: (a) cast from benzene (V_b/V_c = 10/0); (b) cast from cyclohexane (V_b/V_c = 0/10).

the inverted phase observed in this work could be related to such a PL phase, since at first sight it looks very similar. In the PL phase, a continuous PS layer was perforated by isolated PB channels, wherein the hexagonally packed dark spots (PB) were present in the film surface, while for the inverted phase (Figure 1a,d, Figures 2a, 3a, and Figures 4a, 5a), it is apparent in the images that the majority PB domains take up more than 50% of the total area (PB, ~70 wt %). Obviously, both structures have qualitatively different appearance in the surface; moreover, in our previous study,[9] a cross-sectional view of this inverted phase also did not show any sign of layered structure. Thereby, we believe that the inverted phase is not related to the PL structure observed in the thin films as well as in the bulk.[31] On the other hand, by simulations and experiments, they proved that the PL structure is mainly governed by the interplay between surface fields and confinement effects, since the majority PB block with the lower surface energy accumulated at the sample surface, thereby depleting the center of the film. In contrast, our system, the inverted phase of as-cast films evidently depends on the nature of casting solvents. Although, in thin films, on the basis of surface energy considerations, the PB block with the lower surface energy should preferentially segregate at the surface,[59] depending on the nature of solvent used in the casting process; the surface effect can be considered to be hindered by the preferential affinity of the PS block chains for the solvent. Such preferential interactions also control the relative interfacial energy of PS and PB blocks, which may modify the microdomain morphology with respect to the film surface.

Returning to our results, it clearly shows that inverted phase structures are strongly influenced by the nature of the solvent and block copolymer solution concentration, φ. If the solvent exhibits a slight preferential affinity for minority PS block, the solvent will partition preferentially to PS domain and hence swollen more than PB domain. Correspondingly, the system changes the effective volume fraction of each domain and hence alters the curvature of the interface. If the volume fraction of swollen PS matrix is sufficiently high, it will drive the system to form inverted phase at a given solution concentration. Therefore, we deem that the inverted phase frozen-in at the present study is, indeed, the case. On the other hand, toluene and benzene are still good solvents for both PS and PB blocks, and the difference between polymer−solvent interaction parameter for each block is quite small. Because of such weak driving force, we infer that with increasing block copolymer solution concentration the effective volume also changes; consequently, the volume fraction of minority block, f, dominates the interfacial curvature, which induces the inverted phase to transform back to the normal phase structure. This has been evidenced for films cast from toluene, since the inverted phase only observed at short time scale. As time progresses, the polymer chains should have enough time to rearrange to the equilibrium microstructures before immobilization of the system. In this work, the detection is only focused on the microdomain structures presented in thin films. In the other submitted paper, by dynamic laser light scattering the chain dynamics of SBS triblock and

SB diblock copolymers in both dilute and semidilute toluene solutions will be investigated in detail. Although according to theoretical study by Huang and Lodge,[40] the phase transition from inverted to normal phase should be expected when the difference between two polymer−solvent interaction parameters is large enough; nevertheless, as a time-dependent process, the phase transition can involve temporal information and may display kinetic control. Therefore, the inverted phase, as a transient phase, observed in this work is dynamically controlled by matching solvent evaporation rate with phase transformation between inverted and normal phase, which can be detected as long as the time of relaxation is compatible with those of the experimental observations. In the future, we are engaged in similar studies on the SB diblock copolymers where the chain lengths of PS and PB are reversed, i.e., ∼30 wt % PB. We intuitively expect that the obtained phase structures can present a striking contrast with this work, which may provide further insight into the interesting phase behaviors.

Conclusion

The effects of casting solvents on the formation of inverted phase of SB diblock copolymer and matching SBS triblock copolymer having equal polystyrene (PS) weight fraction (about 30 wt %) have been investigated in films cast from different types of solvents: toluene, benzene, cyclohexane, and binary solvent mixture of benzene and cyclohexane. By the freeze-drying method, we were able to successfully freeze-in microstructures of solution-cast films at different time under extremely slow evaporation rates, which correspondto frozen-in phase structures at qualitatively different block copolymer concentrations, φ. In terms of the calculated polymer−solvent interaction parameters (χ) for each block, toluene and benzene are preferential affinity for minority PS block, while cyclohexane is preferential affinity for majority PB block. For films cast from toluene, it was found that the phase transition from inverted phase (i.e., PB spheres or cylinders in a PS matrix) to normal phase (i.e., PS cylinders in a PB matrix) was obtained as a function of time. Further comparing the phase structures cast from benzene, cyclohexane, and their binary solvent mixtures at a given time, progressive changes occur that the inverted phase is not presented with decreasing the solvent affinity for the minority PS block. Our results indicate that the preferential affinity of solvent for the minority PS block, which alters the effective volume fraction of that domain, results in the formation of inverted phase.

Acknowledgment. We are grateful to Dr. Ophelia K. C. Tsui at Physics Department of Hong Kong University of Science and Technology for helpful discussions. This work was supported by the National Science Foundation of China.

References and Notes

(1) Henkee, C. S.; Thomas, E. L.; Fetters, L. J. *J. Mater. Sci.* **1988**, *23*, 1685.
(2) Karim, A.; Singh, N.; Sikka, M.; Bates, F. S.; Dozier, W. D.; Felcher, G. P. *J. Chem. Phys.* **1994**, *100*, 1620.
(3) Radzilowski, L. H.; Carvalho, B. L.; Thomas, E. L. *J. Polym. Sci., Part B: Polym. Phys.* **1996**, *34*, 3081.
(4) Harrison, C.; Park, M.; Chaikin, P. M.; Register, R. A.; Adamson, D. H.; Yao, N. *Polymer* **1998**, *39*, 2733.
(5) Liu, Y.; Zhao, W.; Zheng, X.; King, A.; Singh, A.; Rafailovich, M. H.; Sokolov, J.; Dai, K. H.; Kramer, E. J.; Schwarz, S. A.; Gebizlioglu, O.; Sinha, S. K. *Macromolecules* **1994**, *27*, 4000.
(6) van Dijk, M. A.; van den Berg, R. *Macromolecules* **1995**, *28*, 6773.
(7) Kim, G.; Libera, M. *Macromolecules* **1998**, *31*, 2569; **1998**, *31*, 2670.
(8) Fukunaga, K.; Elbs, H.; Magerle, R.; Krausch, G. *Macromolecules* **2000**, *33*, 947.
(9) Zhang, Q. L.; Tsui, O. K. C.; Du, B.; Zhang, F. J.; Tang, T.; He, T. B. *Macromolecules* **2000**, *33*, 9561.
(10) Knoll, A.; Horvat, A.; Lyakhova, K. S.; Krausch, G.; Sevink, G. J. A.; Zvelindovsky, A. V.; Magerle, R. *Phys. Rev. Lett.* **2002**, *89*, 035501.
(11) Konrad, M.; Knoll, A.; Krausch, G.; Magerle, R. *Macromolecules* **2000**, *33*, 5518.
(12) Hahm, J.; Sibener, S. J. *Langmuir* **2000**, *16*, 4766.
(13) Lammertink, R. G. H.; Hempenius, M. A.; Vancso, G. J. *Langmuir* **2000**, *16*, 6245.
(14) Lammertink, R. G. H.; Hempenius, M. A.; Vancso, G. J.; Shin, K.; Rafailovich, M. H.; Sokolov, J. *Macromolecules* **2001**, *34*, 942.
(15) Fukunaga, K.; Hashimoto, T.; Elbs, H.; Krausch, G. *Macromolecules* **2002**, *35*, 4406.
(16) Elbs, H.; Drummer, C.; Abetz, V.; Krausch, G. *Macromolecules* **2002**, *35*, 5570.
(17) Niu, S.; Saraf, R. F. *Macromolecules* **2003**, *36*, 2428.
(18) Rehse, N.; Knoll, A.; Magerle, R.; Krausch, G. *Macromolecules* **2003**, *36*, 3261.
(19) Knoll, A.; Magerle, R.; Krausch, G. *J. Chem. Phys.* **2004**, *120*, 1105.
(20) Kim, S. H.; Misner, M. J.; Xu, T.; Kimura, M.; Russell, T. P. *Adv. Mater.* **2004**, *16*, 226.
(21) Matsen, M. W. *J. Chem. Phys.* **1997**, *106*, 7781.
(22) Szamel, G.; Müller, M. *J. Chem. Phys.* **2003**, *118*, 905.
(23) Fasolka, M. J.; Banerjee, P.; Mayes, A. M.; Pickett, G.; Balazs, A. C. *Macromolecules* **2000**, *33*, 5702.
(24) Wang, Q.; Nealey, P. F.; de Pablo, J. J. *Macromolecules* **2001**, *34*, 3458.
(25) Huinink, H. P.; Brokken-Zijp, J. C. M.; van Dijk, M. A.; Sevink, G. J. A. *J. Chem. Phys.* **2000**, *112*, 2452.
(26) Huinink, H. P.; van Dijk, M. A.; Brokken-Zijp, J. C. M.; Sevink, G. J. A. *Macromolecules* **2001**, *34*, 5325.
(27) Huang, L.; He, X.; He, T.; Liang, H. *J. Chem. Phys.* **2003**, *119*, 12479.
(28) Horvat, A.; Lyakhova, K. S.; Sevink, J. A.; Zvelindovsky, A. V.; Magerle, R. *J. Chem. Phys.* **2004**, *120*, 1117.
(29) Thurn-Albrecht, T.; Steiner, R.; DeRouchey, J.; Stafford, C. M.; Huang, E.; Bal, M.; Tuominen, M.; Hawker, C. J.; Russell, T. P. *Adv. Mater.* **2000**, *12*, 787.
(30) Thurn-Albrecht, T.; DeRouchey, J.; Russell, T. P.; Jaeger, H. M. *Macromolecules* **2000**, *33*, 3250.
(31) Huang, H.; Zhang, F.; Hu, Z.; Du, B.; He, T.; Lee, F. K.; Wang, Y.; Tsui, O. K. C. *Macromolecules* **2003**, *36*, 4084.
(32) Hanley, K. J.; Lodge, T. P.; Huang, C.-I. *Macromolecules* **2000**, *33*, 5918.
(33) Banaszak, M.; Whitmore, M. D. *Macromolecules* **1992**, *25*, 3406.
(34) Lai, C.; Russel, W. B.; Register, R. A. *Macromolecules* **2002**, *35*, 841.
(35) Hamley, I. W.; Fairclough, J. P.; Ryan, A. J.; Ryu, C. Y.; Lodge, T. P.; Gleeson, A. J.; Pedersen, J. S. *Macromolecules* **1998**, *31*, 1188.
(36) Lodge, T. P.; Xu, X.; Ryu, C. Y.; Hamley, I. W.; Fairclough, J. P. A.; Ryan, A. J.; Pedersen, J. S. *Macromolecules* **1996**, *29*, 5955.
(37) Olvera de la Cruz, M. *J. Chem. Phys.* **1989**, *90*, 1995.
(38) Fredrickson, G. H.; Leibler, L. *Macromolecules* **1989**, *22*, 1238.
(39) Banaszak, M.; Whitmore, M. D. *Macromolecules* **1992**, *25*, 3406.
(40) Huang, C.-I.; Lodge, T. P. *Macromolecules* **1998**, *31*, 3556.
(41) Sadron, C.; Gallot, B. *Makromol. Chem.* **1973**, *164*, 301.
(42) Pico, E. R.; Williams, M. C. *J. Appl. Polym. Sci.* **1978**, *22*, 445.
(43) Gallot, B. *Adv. Polym. Sci.* **1978**, *29*, 87.
(44) Séguéla, R.; Prud'homme, J. *Macromolecules* **1978**, *11*, 1007.
(45) Cohen, R. E.; Bates, F. S. *J. Polym. Sci., Polym. Phys. Ed.* **1980**, *18*, 2143.
(46) Meiners, J. C.; Quintel-Ritzi, A.; Mlynek, J.; Elbs, H.; Krausch, G. *Macromolecules* **1997**, *30*, 4945.
(47) Yu, Y.; Zhang, L.; Eisenberg, A. *Macromolecules* **1998**, *31*, 1144.

(48) Funaki, Y.; Kumano, K.; Nakao, T.; Jinnai, H.; Yoshida, H.; Kimishima, K.; Tsutsumi, K.; Hirokawa, Y.; Hashimoto, T. *Polymer* **1999**, *40*, 7147.
(49) Lodge, T. P.; Hamersky, M. W.; Hanley, K. J.; Huang, C.-I. *Macromolecules* **1997**, *30*, 6139.
(50) Huang, C.-I.; Chapman, B. R.; Lodge, T. P.; Balsara, N. P. *Macromolecules* **1998**, *31*, 9384.
(51) Keller, A.; Pedemonte, E.; Willmouth, F. M. *Kolloid Z. Z. Polym.* **1970**, *238*, 385.
(52) *Polymer Handbook*, 3rd ed.; Brandrup, J., Immergut, E. H., Eds.; John Wiley & Sons: New York, 1989.
(53) *Properties of Polymers*; Van Krevelen, D. W., Ed.; Elsevier Scientific Publishing Co.: Amsterdam, 1976.
(54) Stull, D. R. *Ind. Eng. Chem.* **1947**, *39*, 517.
(55) Leclère, P.; Lazzaroni, R.; Brédas, J. L.; Yu, J. M.; Dubois, P.; Jérôme, R. *Langmuir* **1996**, *12*, 4317.
(56) Bar, G.; Thomann, Y.; Brandsch, R.; Cantow, H.-J.; Whangbo, M.-H. *Langmuir* **1997**, *13*, 3807.
(57) Pico, E. R.; Williams, M. C. *J. Polym. Sci., Phys. Ed.* **1977**, *15*, 1585.
(58) Shultz, A. R.; Flory, P. J. *J. Am. Chem. Soc.* **1952**, *74*, 4760.
(59) Harrison, C.; Paul Chaikin, M. P.; Register, R. A.; Adamson, D. H.; Yao, N. *Macromolecules* **1998**, *31*, 2185.

MA0498621